

Selection of transverse modes in laser cavities containing waveguides and open parts

O V Gurin, A V Degtyarev, V A Maslov, V A Svich, V M Tkachenko, A N Topkov

Abstract. The transverse modes of a submillimetre laser cavity that contains waveguides and open parts were studied theoretically and experimentally with the purpose of finding methods for mode selection. Two methods based on the filtering of the Fourier spectra of the waveguide modes and the use of their interference were substantiated numerically and realised in experiment. Special attention was paid to the mode selection in tunable lasers. Scaling laws allowing one to use the obtained results in a wide range of the cavity parameters and wavelengths are presented.

Keywords: cavity, mode selection, deflecting mirrors, waveguide elements.

1. Introduction

The recent years have witnessed a widespread use of quasi-optical cavities that contain both open and waveguide parts, each of which significantly influences the formation of types of oscillations. Such combined cavities are used in capillary gas-discharge lasers [1], so-called folded waveguide lasers [2], submillimetre (smm) free-electron lasers [3], etc. In a molecular optically pumped laser (OPL), a combined cavity based on a circular metal waveguide was used to realise a broad tuning range (from 0.1 to 1 mm) without replacing the cavity elements and to halve the size of the device [4].

Oversize (multimode) metal waveguides are used in the cavities of millimetre and submillimetre generators to increase the output power, which makes transverse mode selection and realisation of single-mode lasing in such generators an important problem. One can solve this problem by introducing selective losses caused by diffraction in the open parts of the cavity. The authors [5, 6] experimentally studied the mode selection in a smm OPL in the case when a plane mirror was placed in the near-field zone or the Fresnel diffraction zone. It was shown that one could select the mode that was mostly formed by the TE_{01} mode of the metal waveguide. The selective properties of a cavity with spher-

ical mirrors were studied in Ref. [7], where the radii of curvature of the mirrors and the distances between the mirrors and the waveguides that were optimal for selecting the TE_{01} and TE_{02} modes were calculated. However, the main purpose of Ref. [7] was the mode selection with respect to the longitudinal index.

For lasers with a broad tuning range, one should develop methods that would allow technically simple mode selection during the cavity tuning. In this work, we study the transverse mode selection in combined cavities both theoretically and experimentally, using the example of a wide-range compact cavity for a smm OPL that we proposed in Refs [4, 8]. We pay special attention to mode selection in tunable lasers.

2. Theoretical model

The theoretical model of a folded combined cavity (Fig. 1) contains circular metal waveguides 1 and 2, closed at one end with plane mirrors. The waveguides are optically coupled to each other by a system of deflecting mirrors (SDM), which consists of two spherical and one plane mirrors. To simplify the problem, we will consider a cavity that is symmetric with respect to the reflection from the plane mirror of the SDM. The transverse dimensions of the cavity elements are assumed to satisfy the conditions of the quasi-optical and paraxial approximations: $(ka_i)^2 \gg 1$ ($i = 1, 2, 3$), where $k = 2\pi/\lambda$; λ is the wavelength; a_i is the radius of the i th mirror; $k_{\parallel} \gg k_{\perp}$ (the longitudinal wave number is much greater than the transverse one). We will assume that the spherical mirrors are axially symmetric quadratic phase correctors with a focal distance f .

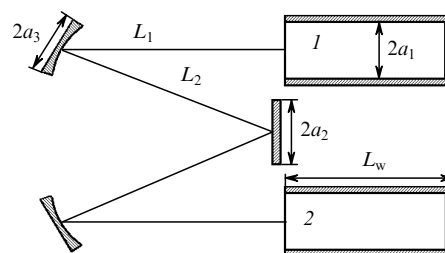


Figure 1. Theoretical model of the combined cavity under study; (1 and 2 are the waveguides).

O V Gurin, A V Degtyarev, V A Maslov, V A Svich, V M Tkachenko, A N Topkov V N Karazin Kharkov National University, pl. Svobody 4, 61077 Kharkov, Ukraine

Received 9 November 2000

Kvantovaya Elektronika 31 (4) 346–350 (2001)

Translated by I V Bargatin

The technique of the numerical calculation of the characteristics of lower cavity modes represents the field in the

waveguides by a superposition of natural waves and the field in the open parts of the cavity by the diffraction integral in the Fresnel approximation. We have performed the calculations for the TE_{0n} and TE_{1n} waves because these waves usually form the output radiation observed in experiments [9, 10].

Up to insignificant constants, the complex amplitudes of the electromagnetic field of the TE_{0n} and TE_{1n} natural waves have the following form at $z = 0$ (the z -axis is directed along the optical axis of the cavity):

$$\begin{aligned} V_{0n}(\rho_1, \varphi) = & -x_0 A_{0n} J_1(\chi_{0n} \rho_1) \sin \varphi \\ & + y_0 A_{0n} J_1(\chi_{0n} \rho_1) \cos \varphi, \end{aligned} \quad (1)$$

$$\begin{aligned} V_{1n}(\rho_1, \varphi) = & x_0 A_{1n} J_2(\chi_{1n} \rho_1) \sin 2\varphi \\ & + y_0 A_{1n} [J_0(\chi_{1n} \rho_1) - J_2(\chi_{1n} \rho_1) \cos 2\varphi], \end{aligned} \quad (2)$$

where x_0 and y_0 are the unit vectors of the Cartesian coordinate axes; $\rho_1 = r/a_1$; r and φ are the cylindrical coordinates;

$$A_{0n} = \frac{1}{J_0(\chi_{0n})\sqrt{\pi}}; \quad A_{1n} = \frac{1}{J_2(\chi_{1n})[2\pi(\chi_{1n}^2 - 1)]^{1/2}}$$

are normalisation factors; J_j is the j th-order Bessel function of the first kind; χ_{mn} is the n th root of the equation $J'_m(\chi) = 0$; $j = 0, 1, 2$; $m = 0, 1$.

Functions V_{mn} satisfy the normalisation condition:

$$\begin{aligned} & \int_0^{2\pi} \int_0^1 V_{nm}(\rho_1, \varphi) V_{kp}(\rho_1, \varphi) \rho_1 d\rho_1 d\varphi \\ & = \begin{cases} 1, & m = k, n = p, \\ 0, & m \neq k \text{ или } n \neq p. \end{cases} \end{aligned} \quad (3)$$

The dependence of the amplitudes on z is given by

$$V_{mn}(\rho_1, \varphi, z) = V_{mn}(\rho_1, \varphi) \exp(i\gamma_{mn}z), \quad (4)$$

where $\gamma_{mn} = \beta_{mn} + i\alpha_{mn}$ is the propagation constant of the natural wave.

Following Ref. [9], we write the expressions for β_{mn} and α_{mn} in the form

$$\beta_{mn} = \left[\left(\frac{2\pi}{\lambda} \right)^2 - \left(\frac{\chi_{mn}}{a_1} \right)^2 \right]^{1/2}, \quad (5)$$

$$\alpha_{mn} = \frac{R_s}{\eta a_1} \left[\frac{m^2}{\chi_{mn}^2 - m^2} + \left(\frac{\lambda \chi_{mn}}{2 \pi a_1} \right)^2 \right] \left[1 - \left(\frac{\lambda \chi_{mn}}{2 \pi a_1} \right)^2 \right]^{-1/2},$$

where $\eta = 376.73 \Omega$ is the wave impedance of free space; R_s is the surface resistance of the waveguide material; equal to $2.61 \times 10^{-7} (c/\lambda)^{1/2} \Omega$ for copper; c is the speed of light in vacuum.

We will search for the field amplitude of the beam incident on the open end of waveguide 1 ($z = 0$) in the form

$$U(\rho_1, \varphi) = \sum_n^N C_n V_{mn}(\rho_1, \varphi). \quad (6)$$

Owing to the axial symmetry of the cavity elements, coefficients C_n can be found independently for each class of

natural waves. Since the cavity is symmetrical with respect to the plane mirror of the SDM, the initial field distribution of natural oscillations is reproduced with a coefficient μ upon a round trip inside waveguide 1 and the following trip to the open end of waveguide 2. From the condition of the field reproduction we derive the following system of linear equations for each class of natural waves:

$$\sum_n^N C_n b_{qn} \exp(i2\gamma_{mn}L_w) = \mu C_q, \quad q = 1, \dots, N, \quad (7)$$

where

$$\begin{aligned} b_{qn} = & 2\pi A_{0q} A_{0n} \int_0^1 \int_0^1 J_1(\chi_{0q} \rho'_1) Q_1(\rho_1, \rho'_1) \\ & \times J_1(\chi_{0n} \rho_1) \rho_1 d\rho_1 \rho'_1 d\rho'_1, \quad m = 0; \end{aligned} \quad (8)$$

$$\begin{aligned} b_{qn} = & 2\pi A_{1q} A_{1n} \int_0^1 \int_0^1 [J_0(\chi_{1q} \rho'_1) Q_0(\rho_1, \rho'_1) J_0(\chi_{1n} \rho_1) \rho_1 \\ & + J_2(\chi_{1q} \rho'_1) Q_2(\rho_1, \rho'_1) J_2(\chi_{1n} \rho_1)] \rho_1 d\rho_1 \rho'_1 d\rho'_1, \quad m = 1; \end{aligned}$$

$$Q_j(\rho_1, \rho'_1) = \int_0^1 Q_j(\rho_2, \rho'_1) Q_j(\rho_1, \rho_2) \rho_2 d\rho_2; \quad (9)$$

where $\rho'_1 = r/a_1$ is the dimensionless coordinate at the open end of waveguide 2. Up to a constant phase factor, the kernels of the integral transformations are given by

$$\begin{aligned} Q_j(\rho_p, \rho_{3-p}) = & -4\pi^2 N_0 \frac{N_p}{1 - \gamma_{3-p}} \exp[i\pi(N_1 \rho_1^2 + N_2 \rho_2^2)] \\ & \times \int_0^1 \exp(i\pi N_0 Z \rho_3^2) J_j(2\pi N_1 \xi_1 \rho_1 \rho_3) J_j(2\pi N_2 \xi_2 \rho_2 \rho_3) \rho_3 d\rho_3, \end{aligned} \quad (10)$$

where $\rho_2 = r/a_2$ and $\rho_3 = r/a_3$ are the dimensionless coordinates on the plane and spherical mirrors;

$$N_0 = \frac{a_3^2}{\lambda f}; \quad N_p = \frac{a_p^2}{\lambda L_p}; \quad Z = \frac{1 - \gamma_1 \gamma_2}{(1 - \gamma_1)(1 - \gamma_2)};$$

$$\gamma_p = 1 - \frac{L_p}{f}; \quad \xi_p = \frac{a_3}{a_p}; \quad p = 1, 2.$$

By solving system of equations (7), we obtain N eigenvalues μ and as many eigenvectors, whose components are the coefficients of the expansion of the cavity modes in waveguide modes. The magnitude of $|C_n|^2$ determines the fraction of the mode energy that is transferred by the TE_{mn} wave. The relative energy loss and the additional round-trip phase shift, which is to be added to the geometrical-optical phase, are given by expressions

$$\delta = 1 - |\mu|^4, \quad \Phi = 2 \arctan \frac{\text{Im} \mu}{\text{Re} \mu}, \quad (11)$$

respectively.

It can be shown that if we set $L_1 = L_2 = f$ in expressions (9) and (10) and let the upper integral limits (apertures of mirrors) tend to infinity, the field distribution of the beam will be transferred distortion-free from one waveguide to the other [8]. This is because each of the phase correctors performs the exact Fourier–Bessel integral transformation of the beam during its transfer from one focal plane to the

other [11]. The characteristic size of the beam on the plane mirror of the SDM (in the region of the Fourier transform) equals the product of the angle of divergence of the beam in the far-field diffraction zone, which is proportional to λ/a_1 , and the focal distance f . By decreasing the radius of the plane mirror a_2 , we can expect the suppression of modes formed by higher waves of the waveguide because the angle of divergence of these waves increases with increasing transverse indices m and n .

If we set $L_2 = f$, $L_1 \geq f$ in (9) and (10) for infinite mirror apertures, the plane of the initial distribution of the beam and the plane of its reproduction will shift from waveguides 1 and 2, respectively, by a distance of $L_1 - f$. Thus, the effect of the SDM on the cavity modes will be equivalent to that of a stretch of free space of length $2(L_1 - f)$ inserted between the waveguides. Since the energy loss due to the diffraction in this stretch increases with increasing transverse mode indices [10], one should expect the selection of lower modes.

3. Results of calculations

The dependence of the energy loss of cavity modes on a_2 and L_1 was calculated numerically according to formulas (7)–(11). We chose the model geometrical dimensions of the cavity to be close to those of a cavity of a small wide-range smm OPL ($a_1 = 9.9$ mm, $L_w = 425$ mm, $f = 80$ mm, $a_3 = 21$ mm, and the material of the waveguides is copper).

We performed the calculation for the extreme wavelengths of the smm range at $\lambda = 0.1$ and 1 mm, and also at $\lambda = 0.4326$ mm, which is the lasing wavelength of the formic-acid OPL pumped by a CO₂ laser on the 9R(20) transition. The number N of expansion terms in formula (7) is determined by the required accuracy of the calculation and was chosen to be 20.

Fig. 2 shows the calculated losses for the four modes that have the highest Q factors as functions of the dimensionless parameter $N_{12} = a_1 a_2 / \lambda f$ for $L_1 = L_2 = f$. The calculation of $|C_n|^2$ has shown that more than 99.5% of each cavity mode is formed by one of the waveguide eigenmodes. This is why we labelled the types of cavity oscillations by the designations of the corresponding waveguide modes. The losses curves that correspond to different λ are not identical owing to the difference in the waveguide losses and the limitation of the beam by the apertures of the spherical mirrors. The greatest difference is observed for the TE₁₁ mode, whose waveguide losses are maximum.

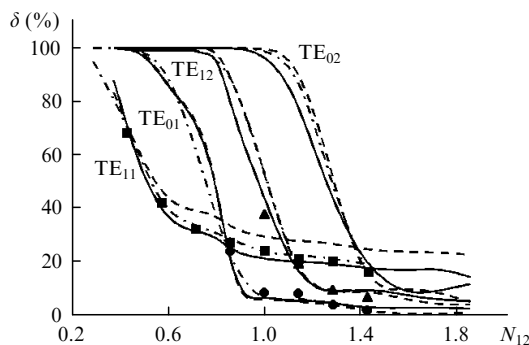


Figure 2. Theoretical (curves) and experimental (points) dependences of the losses for the TE₁₁, TE₀₁, TE₁₂, and TE₀₂ modes on N_{12} for $\lambda = 0.1$ (solid curves), 0.4326 (dashed curves and points), and 1.0 mm (dot-and-dash curves).

At $N_{12} < 0.8$, the TE₁₁ mode is selected; however, the losses for this mode exceed 25%. They can be reduced by increasing the waveguide diameter, but the applicability conditions of the Fresnel approximation will then require such an increase in the system size that all advantages of a waveguide cavity will be lost.

To select the TE₀₁ mode, the parameter N_{12} should be between 0.9 and 1.1. One can increase the losses for the TE₁₁ mode, which has the second-best Q factor, by increasing the waveguide losses. As the frequency of the cavity is tuned, the radius of the plane mirror of the SDM should change proportionally to λ , which can be easily done with the help of an iris diaphragm.

In the case of such a selection of the TE₀₁ mode, its losses amount to 6%, whereas the losses of the mode with the closest Q factor are greater by approximately 20%. This difference can be increased substantially by adjusting the length L_1 of the free-space stretch.

For $L_1 > f$, a sufficiently large aperture a_3 , and $N_{12} = \text{const}$, the behaviour of the oscillation types of the combined cavity is determined by two dimensionless parameters $N_w = \lambda L_w / a_1^2$ and $N_L = \lambda(L_1 - f) / a_1^2$. The parameter N_w determines the difference between the phase shifts of the natural waves that is acquired upon a round trip in the waveguide. If $(\chi_{mm'} / ka_1)^2 \ll 1$, this difference is approximately given by [9]

$$\Delta\varphi_{mm,m'} \approx \frac{N_w}{2\pi} (\chi_{mm'}^2 - \chi_{mm}^2). \quad (12)$$

The parameter N_L is the inverse of the Fresnel number of the free-space stretch of length $L_1 - f$, which is the conventional parameter of diffraction problems. It characterises the beam diffraction inside the SDM. Cavities with coincident parameters N_w and N_L are similar. The possible differences between the characteristics of their modes are due to the same factors as in the case of the above-considered scaling law determined by the parameter N_{12} .

Fig. 3 shows the losses of lower cavity modes as functions of the parameter N_L for different values of the parameter N_w . Note that as N_L increases the cavity modes become less pure, i.e., the number of other natural waves that carry a

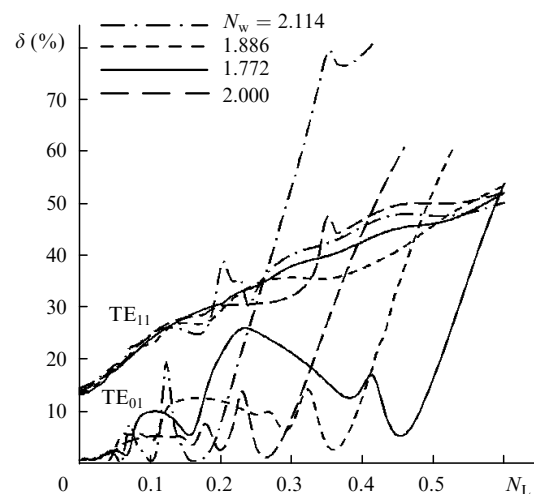


Figure 3. Losses of the TE₁₁ and TE₀₁ modes as functions of N_L for different N_w .

significant fraction of the mode energy increases in expansion (6). The cavity modes are labelled by the indices of the waves that make the greatest contribution. Without significantly limiting the generality of the results, we could perform the calculations for $\lambda = 0.4326$ mm, $a_1 = 9.9$ mm, $a_2 = 10$ mm, $a_3 = 1$ mm, $f = 80$ mm, and varying values of L_1 and L_w .

The general tendency of the obtained dependences is the increase in the losses with increasing N_L , (i.e., with increasing length of the free-space stretch L_1). However, these dependences feature local minima, which are particularly pronounced in the case of the TE₀₁ mode. By our study of the wave content of the TE₀₁ mode showed that, in these minima, the mode is mostly formed by two natural waves. In the rightmost minimum, approximately 20 % (in energy) of the TE₀₂ wave is admixed to the TE₀₁ natural wave; in the next minimum to the left, by about 7 % of the TE₀₃ wave; in the next one, by about 3 % of the TE₀₄ wave, and so on.

The reason for the appearance of minima in the losses is as follows. At some phase shifts of the waveguide modes (12), a convergent beam is formed at the open end of the waveguide. If the curvature of the phase front compensates for the divergence of the beam during its propagation in the free-space stretch of length $2(L_1 - f)$, a minimum in the losses is observed. Our calculations of the phase front confirmed that the losses are minimal when the convergent beam leaving the open end of the waveguide has a spherical phase front, while the entering beam has a plane phase front.

To select the TE₀₁ mode, it is most reasonable to use the minimum with the largest N_L because this maximises the losses of other modes. Since this minimum is mostly determined by the difference between the phase shifts of the TE₀₁ and TE₀₂ waves, we calculated the losses of the cavity modes for $\Delta\varphi_{01,02}$ changing from 2π to 4π with a step of 0.1π , which corresponds to the variation in N_w by 0.0572. We found that if $\Delta\varphi_{01,02}$ lies in the interval between 3.1π and 3.7π (N_w between 1.772 and 2.114), the losses of the TE₀₁ mode in the rightmost minimum of the curve are between 6 and 0.2 %, that is, not larger than in the case of the selection using a diaphragm. As N_w changes from the upper to the lower limit of the interval, the position of the minimum N_L^{\min} shifts from 0.165 to 0.450. In this case, the losses for the

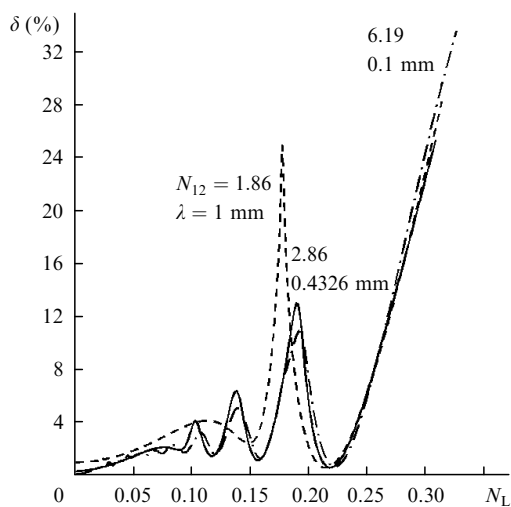


Figure 4. Losses of the TE₀₁ mode as a function of N_L for different N_{12} and $N_w = 2.07$.

TE₁₁ mode, which has the second-best Q factor, at points $N_L = N_L^{\min}$ increase almost monotonically from 25 to 45 %. Thus, compared to the selection using a diaphragm, the selection with the help of a free-space stretch makes it possible to either decrease the losses of the selected mode or suppress the other modes more strongly.

We tested the scaling laws at different wavelengths of the smm range, accordingly changing L_w . Fig. 4 shows the losses of the TE₀₁ mode as a function of N_L for $\lambda = 0.1$, 0.4326, and 1 mm, or $N_{12} = 6.19$, 2.86, and 1.86, respectively, and $N_w = 2.07$. Within the rightmost minimum, even the curves that correspond to different values of N_{12} are close. As N_{12} decreases, the contribution of the upper waves to the cavity mode decreases, and the minima caused by the interference between these waves and the TE₀₁ natural wave gradually disappear.

4. Results of experiment

Fig. 5 shows the structural scheme of the experimental setup for studying the transverse modes of a passive combined cavity and the methods for their selection. The cavity under study 5, with $L_w = 465$ mm, $a_1 = 10$ mm, and $a_3 = 21$ mm, was operated in the transmission regime. An iris diaphragm 7 was used to vary the radius a_2 of the plane mirror of the SDM. All cavity elements were mounted on a IZA-2 measuring line. An electric drive 12 shifted either the semitransparent end reflectors or the SDM precisely along the optical axis, with the misalignment not exceeding 1". Grids made of 25- μ m-wide, 17- μ m-thick nickel bands with a period of 100 μ m served as the semitransparent reflectors. At a wavelength of 0.4326 mm, where the measurements were performed, the transmission coefficient of the grids was 6 %.

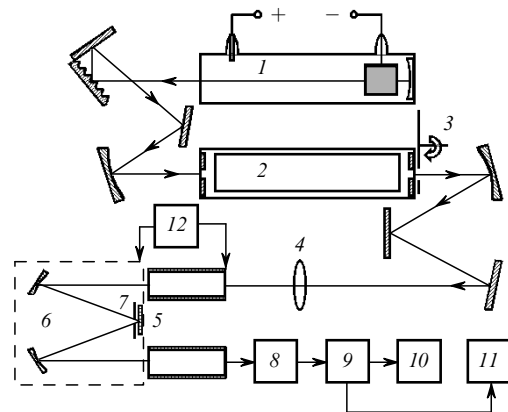


Figure 5. Experimental setup: (1) CO₂ laser, (2) smm cell, (3) beam chopper, (4) lens, (5) combined cavity, (6) SDM, (7) iris diaphragm, (8) pyroelectric transducer, (9) amplifier, (10) oscillograph, (11) recorder, (12) electric drive for the displacement of reflectors and SDM.

The cavity was driven through one of the semitransparent reflectors by the emission of a smm OPL, which consisted of a pumping CO₂ laser 1 and a smm cell 2. The exciting beam was modulated by a beam chopper 3 and matched to the cavity by a quasi-optical circuit and a teflon lens 4 with a focal distance of 30 cm. The radiation transmitted by the cavity was detected by devices 8–11.

The measurement technique was similar to that described in Ref. [10]. The eigenmode spectrum of the cavity

was detected by changing the cavity length with the help of the electric drive 12. The transverse modes were identified using the intermodal intervals calculated from the phase shifts (11) and the well-known theoretical transverse distributions of the intensity and polarisation of waveguide modes. By displacing lens 4 along and perpendicularly to the exciting beam, we maximised the transfer coefficient of the cavity for any given mode. The total energy loss δ_{Σ} per cavity round trip was determined by measuring the width of the resonance curve. The relative error of the loss measurements did not exceed $\pm 5\%$.

From the total losses we distinguished the part δ , given by formula (11), that was due to the diffraction and waveguide losses, and the constant part δ_c that was due to the losses in the reflectors, misalignment of the SDM, etc. The quantity of interest, δ , was calculated from the expression

$$\delta = \frac{\delta_{\Sigma} - \delta_c}{1 - \delta_c}. \quad (13)$$

Obviously, at $\delta \rightarrow 0$ the unknown quantity δ_c coincides with the measured total losses. In the experiment, this was realised by making the diaphragm sufficiently large, so that it no longer contributed to the losses of the TE_{01} mode (the region of $N_{12} > 1.8$ in Fig. 2). The measured value was $\delta_c = 23.5\%$.

The dots in Fig. 2 show the values of δ obtained by measuring the total losses of the TE_{01} , TE_{11} , and TE_{12} modes for the diaphragm radius a_2 varying from 1.5 to 5 mm, which corresponds to the variation in N_{12} from 0.43 to 1.43. At the same time, L_1 and L_2 remained equal to f . The experimental dots are in good agreement with the theoretical curves.

To verify the dependence of the losses on parameter N_L in experiment, we varied the distance L_1 by shifting the SDM as a whole with respect to the waveguides. The diameter of the diaphragm was 10 mm. The dots in Fig. 6 show the measured losses for the TE_{01} and TE_{11} modes. Because of the smallness of the parameter N_{12} , the curve of losses for the TE_{01} mode has one minimum. For comparison, Fig. 6 also shows the theoretical curves. Because the radii of actual waveguides in different sections are known with a low precision, we performed the calculations for $a_1 = 9.9, 10,$ and 10.1 mm. One can see that the concomitant variation in N_w by $\pm 2\%$ significantly shifts the minimum of the losses

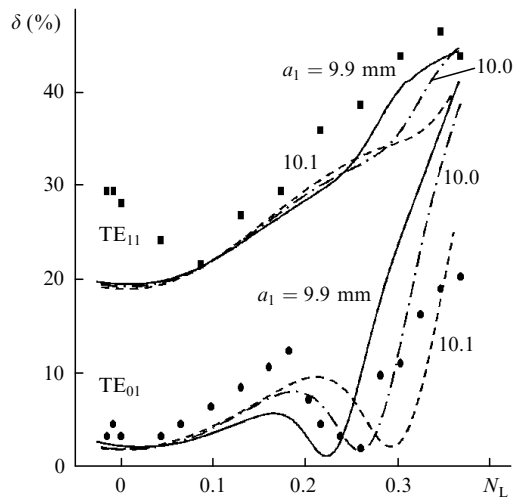


Figure 6. Theoretical (curves) and experimental (dots) dependences of the losses for the TE_{11} and TE_{01} modes on N_L for different a_1 .

along the N_L axis. In this case and also in the case of the frequency tuning of the cavity, the distance L_1 should be optimised to minimise the losses. Generally, the results of the calculation and the experiment are fairly close to each other. The small discrepancy may be caused by the fact that in the calculations we neglected the beam aberrations due to the oblique incidence on the spherical mirrors, imperfections of the waveguides and mirrors, etc.

5. Conclusions

We have proposed and studied two methods for the selection of transverse modes of a combined cavity that are relatively easy to realise in practice. The main advantage of the selection method that uses an iris diaphragm is the possibility to apply this method in a wide range of wavelengths without replacing the cavity elements. The selection method that uses a stretch of free space allows one to increase the efficiency of selecting the TE_{01} mode; however, it is applicable in a limited range of wavelengths that is determined by the waveguide size. Despite the fact that we used the diffraction integral in the Fresnel approximation for the theoretical description of the modes, the results obtained for $N_L \rightarrow 0$ can be interpreted for cavities that contain arbitrarily small stretches of free space. They are also valid for arbitrary cavity sizes and wavelengths provided that the approximations and scaling laws used in this work hold. The underlying principles of the selection methods – the filtering of the spatial Fourier spectrum of waveguide modes and the utilisation of their interference – can be extended to cavities that contain any waveguides.

Note that a selector that consists of a quadratic phase corrector and a back-reflecting plane mirror is in fact sufficient to realise the selection of transverse modes. However, the cavity described above operating in the transmission regime proved to be more convenient for both the experimental studies and the creation of a compact smm laser with optical pumping.

References

1. Abrams R L, Chester A N *Appl. Opt.* **13** 2117 (1974)
2. Jackson P E, Hall D R, Hill C A *Appl. Opt.* **28** 935 (1989)
3. Kleev A I, Manenkov A E *Radiotekh. Elektron.* **33** 1387 (1988)
4. Maslov V A, Svich V A, Tkachenko V M, Topkov A N, Yundev D N *Fiz. Plazmy* **20** 30 (1994) [*Plasma Phys. Rep.* **20** 24 (1994)]
5. Hodges D T, Hartwick T S *Appl. Phys. Lett.* **23** 252 (1973)
6. Gurin O V, Degtyarev A V, Svich V A, Tkachenko V M, Topkov A N *Kvantovaya Elektron.* **24** 33 (1997) [*Quantum Electron.* **27** 31 (1997)]
7. Denisov G G, Lukovnikov D A, Shapiro M A *Radiotekh. Elektron.* **5** 796 (1992)
8. Epishin V A, Ryabykh V N, Tkachenko V M, Topkov A N, Yundev D N RF Patent 2025008 (21 June 1994), *Izobreteniya* (23) 171 (1994)
9. Roser H D, Yamanaka M, Wattenback R, Shultz G V *Intern. J. Infrared Millimeter Waves* **3** 839 (1982)
10. Degtyarev A V, Svich V A, Tkachenko V M, Topkov A N In *Ispol'zovanie radiovoln millimetrovogo i submillimetrovogo diapazonov* (Use of Radio Waves of Millimetre and Submillimetre Bands) (Khar'kov: Institute of Radioelectronics, Academy of Sciences of Ukraine, 1993) p. 105
11. Goodman J *Introduction to Fourier Optics* (New York: McGraw-Hill, 1968; Moscow: Mir, 1970)